

Title: Nanoparticles' and atoms' geometrowave potential quantified and unified properties

Z. R. Tian, Chemistry/Biochemistry, and Materials Science/Engineering, University of Arkansas, Fayetteville, AR 72701, USA, rtian@uark.edu.

This work has introduced a geometrowave potential to linearly fit, consistently unify, and quantitatively predict and compare small particles' geometry-quantized properties both known and new, which complements de Broglie's matter-wave¹. The knowns cover semiconducting nanoparticle (NP) optical bandgap, gold NP's melting point and surface plasmon resonance, and main-group atoms' electronegativity, polarizability, and ionization potential. The new properties include Pauling's unitless electronegativity's substitution, NP-surface atoms' and atom-surface electrons' layering, NPs' surface atoms-shared bonding (like atoms' surface electrons-shared chemical bonding), and countless NP-compounds' nomenclatures, proving the geometrowave potential's general applicability.

For zero-dimensional (0D), 1D-, 2D- and 3D-particles of simple shapes (see the **Extended Data Table S1**), one can quantize their geometry-characterized Surface Area-to-Volume (SA/V) ratio {in the (length⁻¹) unit} into a geometro-wavenumber ($\tilde{\nu}_{GW}$), and their (V/SA) ratio {in the (length) unit} into a geometro-wavelength (λ_{GW}). Hence, the geometro-wave potential (i.e. energy) $\mu_{GW} =$

$hc \cdot \tilde{\nu}_{GW} = hc/\lambda_{GW}$, where the c = speed of light, h = Planck constant, and $hc \approx 1.24$ (keV·nm). The μ_{GW} has helped prove (see below) that the pm- and nm-sized particles' "size-dependent" properties are indeed μ_{GW} -dependent i.e. geometry-quantized.

For semiconductive Cd-X (X = S, Se, Te), for example, their 0D-NPs' optical bandgap energies (E_g) (see the **Extended**

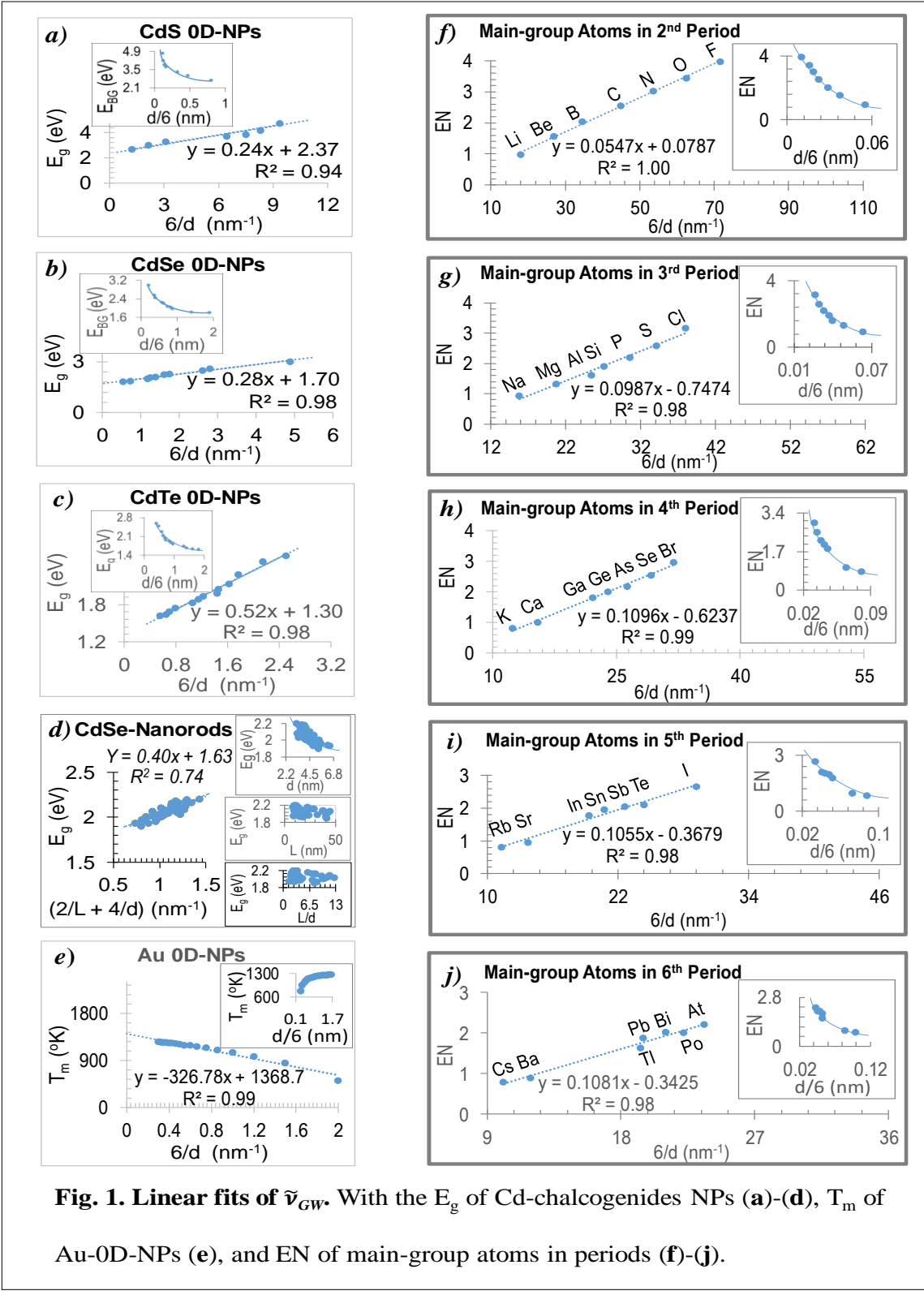


Fig. 1. Linear fits of $\tilde{\nu}_{GW}$. With the E_g of Cd-chalcogenides NPs (a)-(d), T_m of Au-0D-NPs (e), and EN of main-group atoms in periods (f)-(j).

Data Table S2²⁻⁵ fit with their $\tilde{\nu}_{GW}$ (i.e. μ_{GW}/hc) values linearly (**Figs. 1a-1c**) and with

their λ_{GW} (i.e. hc/μ_{GW}) values curvedly (see the insets). Their slopes' trend (i.e. $0.24_{(CdS)}$

$\text{NP}) < 0.28_{(\text{CdSe-NP})} < 0.52_{(\text{CdTe-NP})}$) supports their $E_g(\text{Bulk})$ values' {i.e. $2.42_{(\text{CdS})} > 1.74_{(\text{CdSe})} > 1.50_{(\text{CdTe})}$ (eV)}⁶ and their EN^{7,8}-based bond lengths' {i.e. Cd–S > Cd–Se > Cd–Te}, proving the slope in characterizing each type NP. Logically, the $\tilde{\nu}_{GW}$ and Cd–X bonding energy co-select the adsorbed $\lambda_{(\text{photon})}$. Convincingly, every intercept $\approx E_g(\text{bulk})$ ⁶.

Similarly, CdSe-nanorods' scattering E_g data⁹ (see the **Extended Data Table S3**) fit linearly with their $\tilde{\nu}_{GW}$ values (**Fig. 1d**), proving the μ_{GW} in selectively interacting with a $\lambda_{(\text{photon})}$. Likewise, Au-0D-NPs' melting points¹⁰ (T_m) (see the **Extended Data Table S4**) fit with their $\tilde{\nu}_{GW}$ values linearly (**Fig. 1e**) and λ_{GW} values curvedly (the inset), showing the intercept (1368.7 °K) about 2.3% off the $T_{m(\text{bulk})}$ (1337.3 °K)³. The lower T_m (i.e. higher μ_{GW}) confirms the smaller NP's lower bonding (i.e. lattice) energy that “selects” a longer $\lambda_{(\text{photon})}$ for heating.

Further, 0D-Au-NPs surface plasmon resonance (SPR) wavelengths (λ_{SPR})¹⁰ and

main-group atoms' polarizability⁸ (see the **Extended Data Tables S5-S6**) fit linearly with their λ_{GW} and curvedly with their $\tilde{\nu}_{GW}$ values¹¹ (see the **Extended Data Fig. S1**). These trends support that the μ_{GW} governs the atom- and NP-surfaces' properties generally.

Consistently, every period of main-group atoms' unitless electronegativity (EN) data⁷ fit linearly (**Fig. 1, f-j**) with their $\tilde{\nu}_{GW}$ values and curvedly (the insets) with their λ_{GW} values¹¹ (see the **Extended Data Table S6**). The gap between the *s*- and *p*-orbitals, increasing from **Fig. 1g** to **Fig. 1j** for facilitating the *d*- and then *f*-blocks atoms (omitted here for clarity), revealed the atoms' E_{GW} -generalized and (EN)-complemented periodicity (**Table 1**), and the atoms and NPs layering surfaces' new properties below.

Firstly, main-group atoms' $\tilde{\nu}_{GW}$ fits linearly with their First Ionization Potential (1st IP, critical in Mulliken's EN¹², see the **Extended Data Table S6**) to quantify the atom-surface electrons' μ_{GW} -quantized

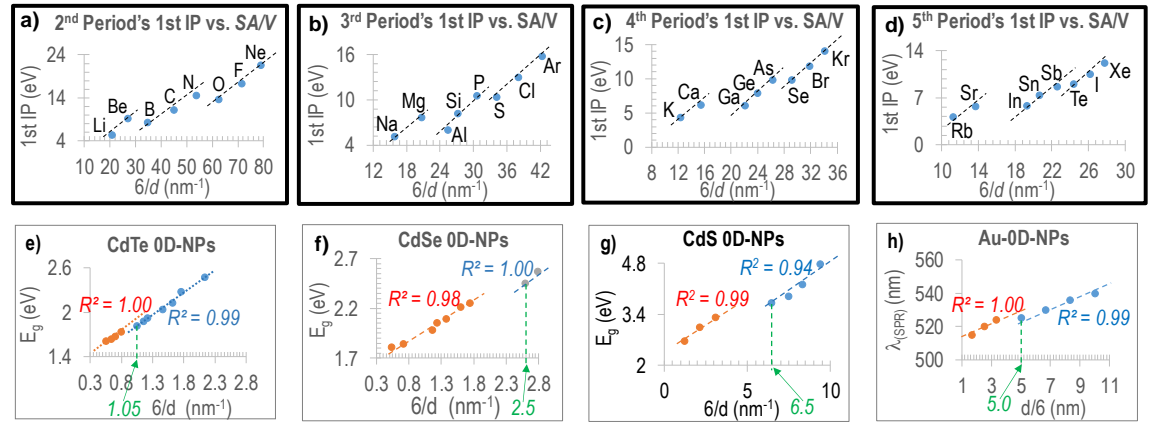


Fig. 2. Atoms' and NPs' structural layering from correlations of their \tilde{v}_{GW} . With main-group atoms

1st IP (a)-(d), with E_g for 0D-NPs of CdTe (e), CdSe (f), and CdS (g), and with Au-0D-NPs $\lambda_{(SPR)}$ (h).

Note: The green dash-lines in (e)-(h) shows the start of the sudden drop in the E_g and $\lambda_{(SPR)}$ values.

layering i.e. in the *s*-orbital first and then the *p*-orbitals before and after the electrons half-fill (**Figs. 2a-2d**). The *s*- and *p*-orbitals' geometrization and quantization in the **Figs. 2a-2d** match that in the **Figs. 1f-1j**. Further, transition metal cations' ionization potential⁸ (see the **Extended Data Table S7**) fits linearly with their \tilde{v}_{GW} (see the **Extended Data Fig. S2**), showing the d-orbital size's negligible change before and after the electrons half-fill.

Likewise, zooming in the **Figs. 1a-1c** has revealed the NPs' sudden (i.e. quantized) E_g drop (see the green dash-lines) as CdTe-NP's (**Fig. 2e**) < CdSe-NP's (**Fig. 2f**) < CdS-

NP's (**Fig. 2g**). This trend supports the PbSe-0D-NPs' negligible E_g drop (see the **Extended Data Table S8** and the **Extended Data Fig. S3**), since the $E_{g(bulk-PbSe)} \approx 0.7$ (eV)⁶ << $E_{g(bulk-CdTe)}$. The E_g 's quantized drop reflects the NP-surface atoms' E_{GW} -quantized layering, like atom-surface electrons' (**Figs. 2a-2d**), revealing the NPs' atomistic nature¹³ which helps expand Bohr's atomic model (i.e. quantum mechanics or QM) to the NP.

Moreover, zooming in the **Extended Data Fig. S1a** has disclosed the Au-0D-NPs' sudden drop of (λ_{SPR}) at $\lambda_{GW} < 4.8$ (nm) (**Fig. 2h**), revealing the Au-NPs' surface atoms layer, too (**Figs. 2e-2g**). The atomistic nature

(**Figs. 2e-2h**) supports smaller NPs' stronger bonding in self-assemblies¹⁴⁻¹⁹ via “sharing” geometrically their surface atoms (see the **Extended Data Fig. S4**), like smaller atoms' stronger inter-bonding via sharing a higher percentage of their surface electrons. This tells that a NP acts like a super atom, and that Bohr's model is generalizable (**Figs. 2a-2d**).

In summary, the new geometrowave potential has been proven generally useful to complement de Broglie's matter-wave (i.e.

QM), and quantitatively predict and compare and consistently unify the NPs and atoms geometry-quantized properties known and new. The new properties, including the NPs' surface-atoms layering, inter-NP bonding, and atoms' EN-complemented and E_{GW} -generalized periodicity, have naturally helped derive new basics for geometrophysics, geochemistry and geochemical biology, which should be detailed separately^{20,21}.

References:

- ¹ de Broglie, L. The Reinterpretation of Wave Mechanics. *Foundations of Physics* **1**, 1 (1970) (<https://link.springer.com/article/10.1007/BF00708650>).
- ² Rossetti, R.; Nakahara, S. and Brus, L. E. Quantum size effects in the redox potentials, resonance Raman spectra, and electronic spectra of CdS crystallites in aqueous solution. *J. Chem. Phys.* **79**, 1086–1088 (1983).(<https://aip.scitation.org/doi/pdf/10.1063/1.445834>).
- ³ Murray, C. B.; Norris and D. J.; Bawendi, M. G. Synthesis and characterization of nearly monodisperse CdE (E = Sulfur, Selenium, Tellurium) semiconductor nanocrystallites. *J. Am. Chem. Soc.* **115**, 8706–8715 (1993). (<https://pubs.acs.org/doi/abs/10.1021/ja00072a025>).
- ⁴ Vossmeier, T.; Katsikas, L.; Giersig, M.; Popovic, I. G.; Diesner, K.; Chemseddine, A.; Eychmueller, A. and Weller, H. CdS Nanoclusters: Synthesis, Characterization, Size Dependent Oscillator Strength, Temperature Shift of the Excitonic Transition Energy, and Reversible Absorbance Shift. *J. Phys. Chem.* **98**, 7665–7673 (1994). (<https://pubs.acs.org/doi/abs/10.1021/j100082a044>).
- ⁵ Yu, W. W.; Qu, L.; Guo, W. and Peng, X. Experimental determination of the extinction coefficient of CdTe, CdSe, and CdS nanocrystals. *Chem. Mater.* **15** (14), 2854–2860 (2003). (<https://pubs.acs.org/doi/abs/10.1021/cm034081k>).
- ⁶ Semiconductor Band Gaps <http://hyperphysics.phy-astr.gsu.edu/hbase/Solids/bandgap.html>.
- ⁷ Pauling, L. *The Nature of the Chemical Bond* (Cornell Univ. Press, Ithaca, 1960). (https://www.academia.edu/26073847/Pauling_L._The_nature_of_the_chemical_bond_Cornell_Univ._1960_).

- ⁸ Lide, D. R. *CRC Handbook of Chemistry and Physics* (CRC Press, Boca Raton, FL, 2000). (<http://diyhpl.us/~nmz787/mems/unorganized/CRC%20Handbook%20of%20Chemistry%20and%20Physics%2085th%20edition.pdf>).
- ⁹ Li, L.-S.; Hu, J.; Yang, W. and Alivisatos, A. P. Band gap variation of size- and shape-controlled colloidal CdSe quantum rods. *Nano Lett.* **1** (7), 349–351 (2001). (<https://pubs.acs.org/doi/10.1021/nl015559r>).
- ¹⁰ *Gold NPs: Properties and Applications*, Sigma-Aldrich, (www.sigmaaldrich.com/technical-documents/articles/materials-science/nanomaterials/gold-nanoparticles.html).
- ¹¹ *Calculated atomic radii* (Ed. Jan-7-2019), ([https://en.wikipedia.org/wiki/Atomic_radii_of_the_elements_\(data_page\)](https://en.wikipedia.org/wiki/Atomic_radii_of_the_elements_(data_page))).
- ¹² Mulliken, R. S. A New Electroaffinity Scale; Together with Data on Valence States and on Valence Ionization Potentials and Electron Affinities. *J. Chem. Phys.* **2** (11): 782–793 (1934). (<https://aip.scitation.org/doi/10.1063/1.1749394>).
- ¹³ Zunger, A. Pseudopotential theory of semiconductor quantum dots. *Phys. Stat. Sol. (b)* **224**, 727–734 (2001). ([https://doi.org/10.1002/\(SICI\)1521-3951\(200104\)224:3<727::AID-PSSB727>3.0.CO;2-9](https://doi.org/10.1002/(SICI)1521-3951(200104)224:3<727::AID-PSSB727>3.0.CO;2-9)).
- ¹⁴ Kresge, C. T.; Leonowicz, M. E.; Roth, W. J.; Vartuli, J. C. and Beck, J. S. Ordered mesoporous molecular sieves synthesized by a liquid-crystal template mechanism. *Nature* **359**, 710-712 (1992). (<https://www.nature.com/articles/359710a0>).
- ¹⁵ Tian, Z. R.; Tong, W.; Wang, J. Y.; Duan, N. G.; Krishnan, V. V. and Suib, S. L. Manganese oxide mesoporous structures: mixed-valent semiconducting catalysts. *Science* **276**, 926 (1997). (<https://science.sciencemag.org/content/276/5314/926>).

- ¹⁶ Yang, P. D.; Zhao, D.; Margolese, D. I.; Chmelka, B. F. and Stucky, G. D. Generalized syntheses of large-pore mesoporous metal oxides with semicrystalline frameworks. *Nature* **396**, 152-155 (1998). (<https://www.nature.com/articles/24132>).
- ¹⁷ Whitesides, G. W. and Grzybowski, B. Self-assembly at all scales. *Sci.* **295**, 2418–2421 (2002). (<https://science.sciencemag.org/content/295/5564/2418.full>).
- ¹⁸ Aizenberg, J.; Weaver, J. C.; Thanawala, M. S.; Sundar, V. C.; Morse, D. E. and Fratzl, P. Skeleton of Euplectella sp.: structural hierarchy from the nanoscale to the macroscale. *Science* **309**, 275-278 (2005). (DOI: [10.1126/science.1112255](https://doi.org/10.1126/science.1112255)).
- ¹⁹ Hua, L; Zheng, J.; Zhou, Z. R.; and Tian, Z. R. Water-Switchable Interfacial Bonding on Tooth Enamel Surface, *ACS Biomater. Sci. Eng.* **4** (7), 2364–2369 (2018). (<https://pubs.acs.org/doi/full/10.1021/acsbiomaterials.8b00403>).
- ²⁰ Tian, Z. R. Geometry-Wave Potential Quantified and Unified Properties in General Chemistry. ChemRxiv. Preprint (2019). <https://doi.org/10.26434/chemrxiv.9759581.v4>.
- ²¹ Tian, Z. R. Surface curvature-quantized energy and forcefield in spacetime-warped chemical physics. ChemRxiv. Preprint (2020). <https://doi.org/10.26434/chemrxiv.11495811.v3>.

Acknowledgement: The author acknowledges H. W. Kroto, J. T. Yates, Z. L. Wang, P. Pulay, C. D. Heyes, H. C. Tian, and H-J. Zhao for helpful discussions in this five-year “big data” work.

SUPPLEMENTARY DATA.

I. Extended Data Tables S1–S8.

II. Extended Data Figures S1–S3.

Title: **Nanoparticles' and atoms' geometrowave potential quantified and unified properties**

Z. R. Tian, Chemistry/Biochemistry, and Materials Science/Engineering, University of Arkansas, Fayetteville, AR 72701, USA, rtian@uark.edu.

I. Extended Data Tables.

1). Extended Data Table S1.

Table S1. Simple-Shape Particles' \tilde{v}_{GW} and Point Group of Symmetry					
	Shape	Surface-Area (SA)	Volume (V)	$\tilde{v}_{GW} (= SA/V)$	PntGrpSym
0D	 d	πd^2	$\pi d^3/6$	$(6/d)^*$	R_3
1D	 d	$4dL + 2d^2$	$d^2 L$	$(4/d + 2/L)**$ or $(4/d)**$ if $d \ll L$	D_{4d}
	 d	$\pi d^2/2 + \pi dL$	$\pi d^2 L/4$	$(4/d + 2/L)**$ or $(4/d)**$ if $d \ll L$	$D_{\infty d}$
2D	 d	$\pi D^2/2 + d\pi D$	$d\pi D^2/4$	$2/d + 4/D;$ or $2/d$ if $d \ll D$	$D_{\infty d}$
	 d	$2(aL + aL + L^2)$	aL^2	$2/d + 2/L + 2/a;$ or $2/d$ if $d \ll L$	D_{4d}
3D	 d	$6d^2$	d^3	$(6/d)^*$	O_h
	 d	$2 \times 3^{1/2} d^2$	$2^{1/2} d^3/3$	$3(6^{1/2})/d$	O_h
	 d	$1.732 d^2$	$0.118 d^3$	$14.678/d$	T_d

*The spherical and cubic particles share the same \tilde{v}_{GW} formula;
**The 1D-particles share the same \tilde{v}_{GW} formula.

2). Extended Data Table S2.

Table S2. Semiconducting 0D-NPs E_g and $\tilde{\nu}_{GW}$								
(a). CdS 0D-NP			(b). CdSe 0D-NP			(c). CdTe 0D-NP		
E_{BG} (eV)	d/6 (nm)	6/d (nm $^{-1}$)	E_{BG} (eV)	d/6 (nm)	6/d (nm $^{-1}$)	E_{BG} (eV)	d/6 (nm)	6/d (nm $^{-1}$)
4.78	0.11	9.4	3.00	0.205	4.9	2.58	0.4	2.5
4.22	0.12	8.3	2.57	0.358	2.8	2.48	0.47	2.1
3.89	0.14	7.5	2.45	0.393	2.6	2.28	0.57	1.8
3.72	0.16	6.5	2.25	0.575	1.7	2.13	0.62	1.6
3.32	0.32	3.1	2.21	0.624	1.6	2.04	0.68	1.5
3.05	0.47	2.1	2.09	0.727	1.4	1.97	0.71	1.4
2.68	0.80	1.3	2.05	0.807	1.2	1.93	0.82	1.2
			1.98	0.860	2.2	1.88	0.87	1.2
			1.84	1.39	0.72	1.82	0.95	1.1
			1.61	1.88	0.53	1.74	1.3	0.79
						1.68	1.4	0.70
						1.64	1.6	0.64
						1.62	1.8	0.55

3). Extended Data Table S3.

Table S3. Au-0D-NPs melting points and $\tilde{\nu}_{GW}$					
d/6 (nm)	6/d (nm $^{-1}$)	T_m (°K)	d/6 (nm)	6/d (nm $^{-1}$)	T_m (°K)
0.30	3.330	773	1.05	5.714	1223
0.38	15.79	953	1.13	5.301	1233
0.47	12.77	1043	1.22	4.918	1243
0.55	10.91	1098	1.30	4.615	1251
0.64	9.375	1138	1.38	4.349	1255
0.72	8.333	1163	1.45	4.138	1256
0.80	7.500	1183	1.53	3.922	1262
0.88	6.818	1198	1.62	3.704	1266
0.95	6.316	1208			

4). Extended Data Table S4.

Table S4. Semiconducting CdSe-Nanorod E_g and $\tilde{\nu}_{GW}$									
E_g (eV)	d (nm)	L (nm)	L/d	(SA / V)* (nm ⁻¹)	E_g (eV)	d (nm)	L (nm)	L/d	(SA / V)* (nm ⁻¹)
2.20	3.2	11.0	3.4	1.4	2.07	4.3	8.7	2.0	1.2
2.08	3.3	37.8	12	1.27	2.08	4.3	16.4	3.8	1.1
2.03	3.4	43.1	13	1.23	2.10	4.4	8.6	2.0	1.1
2.11	3.5	28.0	8.0	1.2	1.98	4.4	31.5	7.2	0.97
2.05	3.5	38.5	11	1.2	2.10	4.5	15.3	3.4	1.0
2.17	3.6	11.5	3.2	1.3	2.02	4.6	19.8	4.3	0.97
2.16	3.6	22.1	6.1	1.2	1.97	4.6	19.8	4.3	0.97
2.16	3.7	7.6	2.1	1.3	2.03	4.8	12.4	2.6	0.99
2.19	3.7	9.2	2.5	1.3	2.03	4.8	19.4	4.0	0.94
2.12	3.7	26.1	7.1	1.2	1.93	4.8	40.4	8.4	0.88
2.12	3.7	28.8	7.8	1.2	2.06	4.9	18.4	3.8	0.93
2.12	3.8	8.6	2.3	1.3	2.06	4.9	18.9	3.9	0.92
2.07	3.9	37.2	9.5	1.1	1.99	5.1	12.0	2.4	0.95
2.06	3.9	44.3	11	1.1	2.00	5.2	11.4	2.2	0.94
2.12	4.0	9.7	2.4	1.2	2.00	5.2	22.2	4.3	0.86
2.18	4.0	11.6	2.9	1.2	1.90	5.3	40.8	7.7	0.80
2.02	4.0	41.3	10	1.1	2.00	5.4	18.2	3.4	0.85
2.15	4.1	12.7	3.1	1.1	1.95	5.5	8.5	1.6	0.96
2.13	4.1	13.4	3.3	1.1	1.96	5.5	18.4	3.4	0.84
2.04	4.1	16.9	4.1	1.1	1.97	5.5	23.6	4.3	0.81
2.00	4.1	40.2	9.8	1.0	1.94	6.2	14.0	2.3	0.79
2.06	4.2	16.5	3.9	1.1	1.93	6.4	17.6	2.8	0.74
2.02	4.2	20.2	4.8	1.1					

* (SA/V) = (2/L) + (4/d), from the Table 1

5). Extended Data Table S5.

Table S5. Au-0D-NP's λ_{GW} , $\tilde{\nu}_{GW}$ and λ_{SPR}			
d (nm)	$\lambda_{QGD} = d/6$ (nm)	$\tilde{\nu}_{QGD} = 6/d$ (nm ⁻¹)	λ_{SPR} (nm)
10	1.67	0.60	517.5
15	2.5	0.40	520
20	3.33	0.30	524
30	5	0.20	526
40	6.67	0.15	530
50	8.33	0.12	535
60	10	0.10	540
80	13.33	0.075	553
100	16.67	0.060	572

6). Extended Data Table S6.

Table S6. Main-group atoms polarizability, electronegativity, 1st IP, and $\tilde{\nu}_{GW}$

Atom	Polarizability ⁽³⁾ (10^{-24} cm^3)	EN ⁽³⁾ (eV)	1st IP ⁽³⁾ (eV)	d/6 ^{(3),(11)} (nm)	6/d (nm ⁻¹)	Atom	Polarizability ⁽³⁾ (10^{-24} cm^3)	EN ⁽³⁾ (eV)	1st IP ⁽³⁾ (eV)	d/6 ^{(3),(11)} (nm)	6/d (nm ⁻¹)
H	0.667	2.2	13.598	0.0177	56.6	Ge	6.07	2.01	7.899	0.0417	24.0
He	0.205		24.587	0.0103	96.8	As	4.31	2.18	9.789	0.038	26.3
Li	24.3	0.98	5.391	0.0555	18.0	Se	3.72	2.55	9.752	0.0342	29.2
Be	5.6	1.57	9.322	0.0373	26.8	Br	3.05	2.96	11.814	0.0313	31.9
B	3.03	2.04	8.298	0.029	34.5	Kr	2.48		14.0	0.0293	34.1
C	1.76	2.55	11.26	0.0223	44.8	Rb	47.3	0.82	4.177	0.0885	11.3
N	1.1	3.04	14.534	0.0187	53.6	Sr	27.6	0.95	5.695	0.073	13.7
O	0.802	3.44	13.618	0.016	62.5	In	10.2	1.78	5.786	0.0518	19.3
F	0.557	3.98	17.423	0.01	71.5	Sn	7.7	1.96	7.344	0.0483	20.7
Ne	0.39		21.565	0.0127	78.9	Sb	6.6	2.05	8.608	0.0442	22.6
Na	24.08	0.93	5.139	0.0633	15.8	Te	5.5	2.1	9.01	0.041	24.4
Mg	10.6	1.31	7.646	0.0483	20.7	I	5.35	2.66	10.451	0.0342	29.2
Al	6.8	1.61	5.986	0.0393	25.4	Xe	2.6	2.6	12.13	0.036	27.8
Si	5.38	1.90	8.152	0.0369	27.1	Cs	59.6	0.79	3.894	0.099	10.1
P	3.63	2.19	10.487	0.0327	30.6	Ba	39.7	0.89	5.212	0.084	11.9
S	2.9	2.58	10.36	0.0293	34.1	Tl	7.6	1.8	6.108	0.0623	15.8
Cl	2.18	3.16	12.968	0.0263	38.0	Pb	6.8	1.8	7.417	0.0513	19.5
Ar	1.62		15.76	0.0236	42.3	Bi	7.4	1.9	7.286	0.0476	21.0
K	43.3	0.82	4.341	0.0806	12.4	Po	6.8	2.0	8.417	0.045	22.2
Ca	22.8	1.00	6.113	0.0645	15.5	At	6.0	2.2		0.0424	23.6
Ga	8.12	1.81	5.999	0.0452	22.1	Rn	2.2		10.749	0.040	25.0

Note: The superscripts (3) and (11) represent the References #3 and #11.

7). Extended Data Table S7.

Table S7. High-valent monoatomic cations $\tilde{\nu}_{GW}$ and ionization potentials

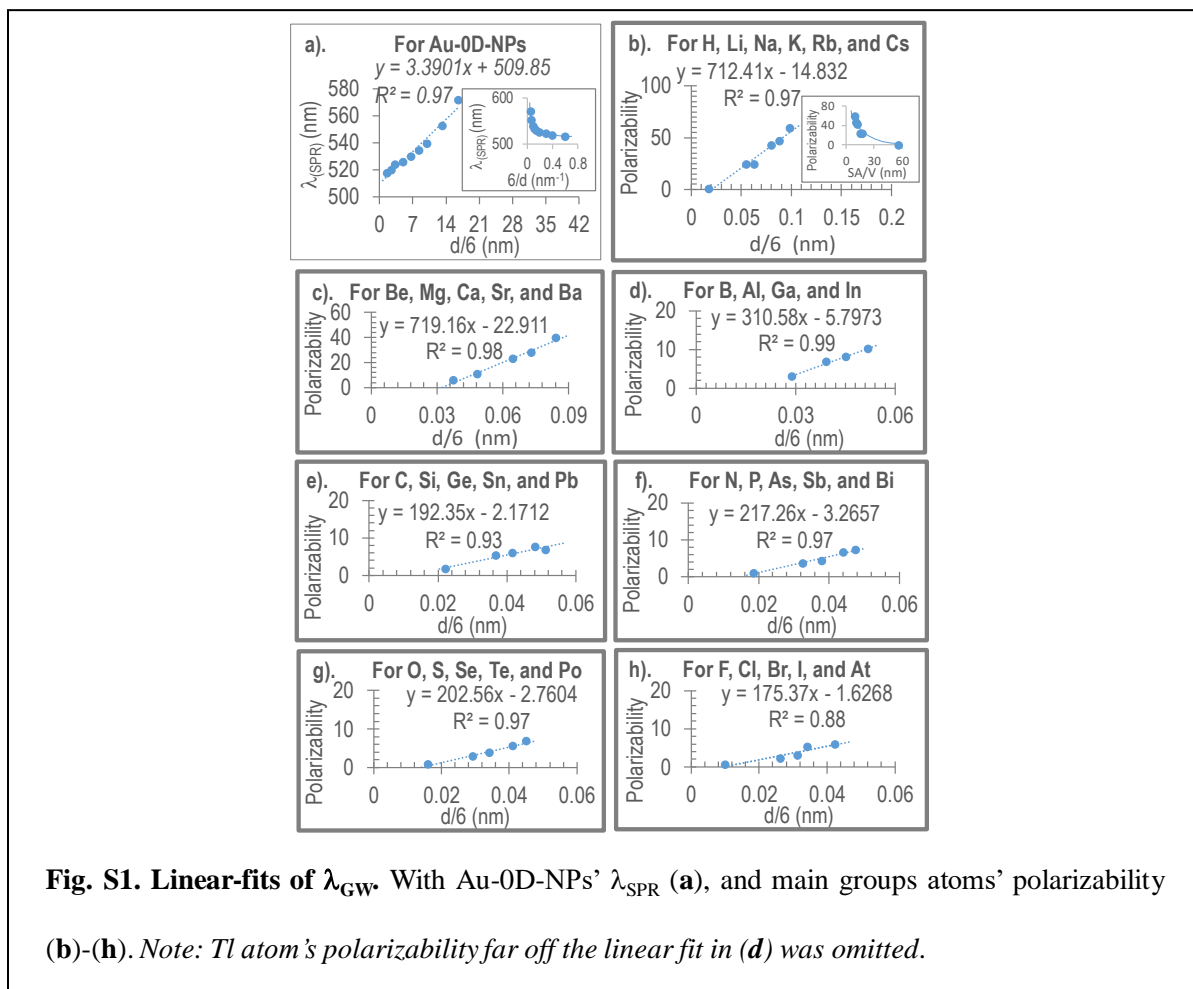
Cation	d/2 (nm)	6/d (nm ⁻¹)	IP (eV)	Cation	d/2 (nm)	6/d (nm ⁻¹)	IP (eV)
V (II)	0.079	37.97	29.311	Mn (II)	0.083	36.14	33.668
V (III)	0.064	46.88	46.71	Mn (III)	0.058	51.72	51.2
V (IV)	0.058	51.72	65.28	Mn (IV)	0.053	56.6	72.4
V (V)	0.054	55.56	128.13	Mn (V)	0.033	90.91	95.6
Cr (II)	0.073	41.1	30.96	Mn (VI)	0.026	115.38	119.203
Cr (III)	0.062	48.39	49.16	Mn (VII)	0.025	120	194.5
Cr (IV)	0.055	54.55	90.635	Mo (III)	0.069	43.48	46.4
Cr (VI)	0.044	68.18	160.18	Mo (IV)	0.065	46.15	54.49
				Mo (V)	0.061	49.18	68.83
				Mo (VI)	0.059	50.85	125.67

8). Extended Data Table S8.

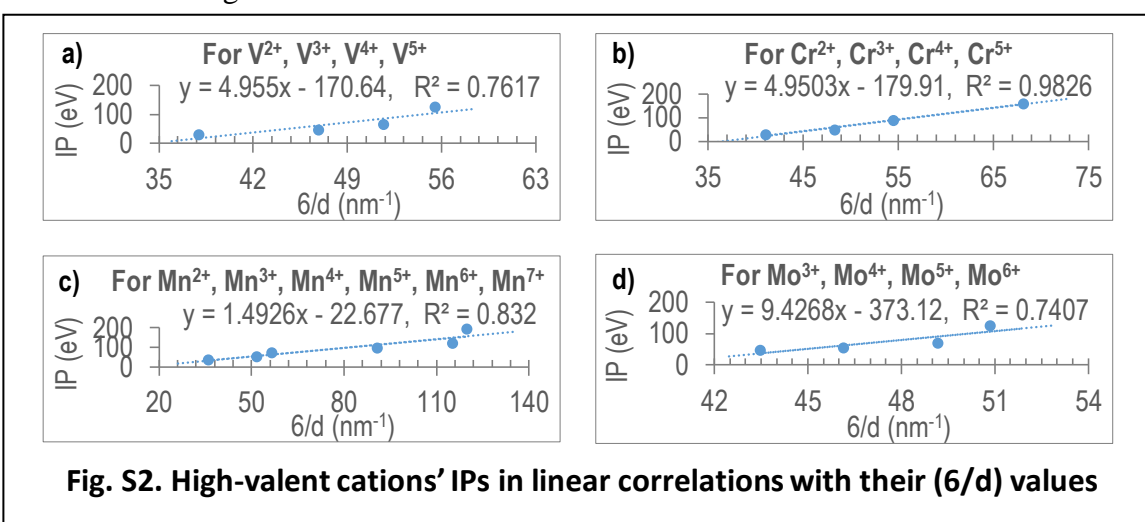
Table S8. PbSe 0D-NP	
E_g (eV)	$6/d$ (nm $^{-1}$)
0.833	1.18
0.967	1.40
1.077	1.58
1.243	1.88
1.656	2.61

II. Extended Data Figures:

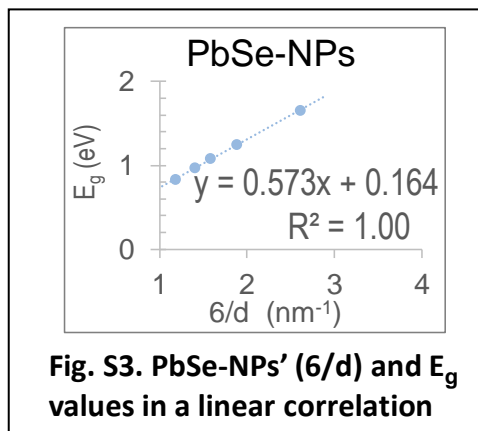
1). Extended Data Fig. S1.



2). Extended Data Fig. S2.



3). Extended Data Fig. S3.



4). Extended Data Fig. S4.

